



HAL
open science

Structure-function relationships for *Schizophyllum commune* trehalose phosphorylase and their implications for the catalytic mechanism of family GT-4 glycosyltransferases

Christiane Goedl, Richard Griessler, Alexandra Schwarz, Bernd Nidetzky

► **To cite this version:**

Christiane Goedl, Richard Griessler, Alexandra Schwarz, Bernd Nidetzky. Structure-function relationships for *Schizophyllum commune* trehalose phosphorylase and their implications for the catalytic mechanism of family GT-4 glycosyltransferases. *Biochemical Journal*, 2006, 397 (3), pp.491-500. 10.1042/BJ20060029 . hal-00478505

HAL Id: hal-00478505

<https://hal.science/hal-00478505>

Submitted on 30 Apr 2010

HAL is a multi-disciplinary open access archive for the deposit and dissemination of scientific research documents, whether they are published or not. The documents may come from teaching and research institutions in France or abroad, or from public or private research centers.

L'archive ouverte pluridisciplinaire **HAL**, est destinée au dépôt et à la diffusion de documents scientifiques de niveau recherche, publiés ou non, émanant des établissements d'enseignement et de recherche français ou étrangers, des laboratoires publics ou privés.

Structure-function relationships for *Schizophyllum commune* trehalose phosphorylase and their implications for the catalytic mechanism of family GT-4 glycosyltransferases

Christiane GÖDL, Richard GRIESSLER, Alexandra SCHWARZ and Bernd NIDETZKY*

Institute of Biotechnology and Biochemical Engineering
Graz University of Technology, Petersgasse 12, A-8010 Graz, Austria

* Corresponding author

Dr. Bernd Nidetzky

Institute of Biotechnology and Biochemical Engineering, Graz University of Technology, Petersgasse 12/I, 8010 Graz, Austria

E-mail: bernd.nidetzky@TUGraz.at

Phone: +43-316-873-8400; Fax: +43-316-873-8434

Running title: Recombinant trehalose phosphorylase from *Schizophyllum commune*

Revised version: BJ2006/0029

List of abbreviations

<i>Sc</i> TPase	Trehalose phosphorylase from <i>Schizophyllum commune</i>
<i>Ec</i> MalP	Maltodextrin phosphorylase from <i>E. coli</i>
<i>At</i> GS	Glycogen synthase from <i>Agrobacterium tumefaciens</i>
OtsA	Trehalose 6-phosphate synthase from <i>E. coli</i>
α -D-Glc 1-P	α -D-glucose 1-phosphate
UDP-Glc	UDP- α -D-glucose
S _{Ni} -like mechanism	Internal return-like mechanism
GPGT	Glycogen phosphorylase glycosyltransferase superfamily
LC ESI Q-TOF MS	Liquid chromatography electrospray ionisation quadrupole time-of-flight mass spectroscopy

Numbering of *Sc*TPase starts with the initiator methionine as 1 and does not consider the N-terminal 11 amino acid-long fusion peptide that is used for recombinant protein production.

SYNOPSIS

The cDNA encoding trehalose phosphorylase, a family GT-4 glycosyltransferase from the fungus *Schizophyllum commune*, was isolated and expressed in *Escherichia coli* to yield functional recombinant protein in its full length of 737 amino acids. Unlike the natural phosphorylase that was previously obtained as a truncated 61-kDa monomer containing one tightly bound Mg^{2+} , the intact enzyme produced in *E. coli* is a dimer and not associated with metal ions. MS analysis of the slow spontaneous conversion of the full-length enzyme into a 61-kDa fragment which is fully active revealed that critical elements of catalysis and specificity of trehalose phosphorylase reside entirely in the C-terminal protein part. Intact and truncated phosphorylases thus show identical inhibition constants for the transition state analogue orthovanadate and α,α -trehalose ($K_i \approx 1 \mu M$). Structure-based sequence comparison with retaining glycosyltransferases of fold family GT-B reveals a putative active centre of trehalose phosphorylase, and results of site-directed mutagenesis confirm the predicted crucial role of Asp-379, His-403, Arg-507 and Lys-512 in catalysis and also delineate a function of these residues in determining the large preference of the wild-type enzyme for the phosphorolysis compared with hydrolysis of α,α -trehalose. The pseudo-disaccharide validoxylamine A was identified as a strong inhibitor of trehalose phosphorylase ($K_i = 1.7 \pm 0.2 \mu M$) that displays 350-fold tighter binding to the enzyme-phosphate complex than the non-phosphorolysable substrate analogue α,α -thio-trehalose. Structural and electronic features of the inhibitor that may be responsible for high-affinity binding and their complementarity to an anticipated glucosyl oxocarbenium ion-like transition state are discussed.

Keywords: α -retaining mechanism; glycosyltransferase; GT-B fold; oxocarbenium ion-like transition state; internal return mechanism

INTRODUCTION

Glycosyltransferases catalyze the transfer of a glycosyl moiety from a donor sugar to an acceptor molecule. In the present postgenomic era, there is much interest in elucidating their mechanism and specificity as the molecular determinants of the complexity of natural glycan structures [1, 2]. Eighty-three glycosyltransferase families (as 04/13/06) have been categorized in a sequence-derived classification system [3]. Two basic protein topologies, each one of the Rossmann-fold type, have been observed so far for glycosyltransferases and are commonly termed GT-A and GT-B [1-3].

Mechanistically, the glycosyltransferases can be classified according to whether they retain or invert the anomeric configuration of the donor substrate in the glycosidic product. Enzymatic glycosyl transfer with inversion is thought to occur by a single nucleophilic displacement mechanism that features an oxocarbenium ion-like transition state [4]. The catalytic scenario for retaining glycosyltransferases is conceptually much less clear [5]. Enzymatic hydrolysis of glycosides with retention of configuration involves the formation and subsequent breakdown of an inverted covalent glycosyl-enzyme intermediate [4, 6, 7]. A similar two-step (double-displacement) mechanism was considered probable for retaining glycosyltransferases but in spite of the attempts to delineate the catalytic steps, no convincing support for a covalent intermediate has been obtained so far [4 and refs. therein; 8-10]. This has led to the consideration of alternative scenarios [4, 11, 12] among which the internal return (S_{Ni})-like mechanism [13] seems to be a strong possible choice.

Retaining glycosyl transfer via internal return would involve departure of the leaving group and attack of the nucleophile in a concerted manner from the same side of the glycosyl moiety (Figure 1). A close hydrogen bond between the incoming nucleophile and leaving group would facilitate the S_{Ni} -like reaction, providing stabilization to the anticipated oxocarbenium ion-like transition state that is likely to have a strongly dissociative character.

Further electrostatic stabilization of this transition state could come from the suitably positioned anionic leaving group/nucleophile. Surrounding the catalytic event, the widely observed kinetic scenario for retaining glycosyltransferases in which donor sugar and acceptor must combine in a ternary enzyme-substrate complex before reaction takes place is a *strict requirement* of the S_Ni -like mechanism whereas glycosyl transfer via covalent intermediate is compatible with other kinetic schemes, especially the ping-pong mechanism. While trapping of covalent glycosyl enzyme intermediate is conceptually straightforward, it is very difficult to design experiments that probe internal return.

ScTPase (*Schizophyllum commune* trehalose phosphorylase, EC 2.4.1.231) catalyzes glucosyl transfer to and from phosphate using α,α -trehalose and α -D-Glc 1-P (α -D-glucose 1-phosphate) as the respective donor substrate [14]. Peptide fingerprinting analysis revealed that the enzyme belongs to glycosyltransferase family GT-4 [10]. *ScTPase* has an ordered kinetic mechanism, as indicated in Figure 2A, and the physiological direction of the reaction is the phosphorolysis of α,α -trehalose [10, 14]. Evidence hinting at an S_Ni -type mechanism of retaining glucosyl transfer by *ScTPase* is the transition state-like inhibition by the phosphate analogue vanadate in combination with glucose [15]. A non-covalent adduct of the two enzyme-bound ligands, arguably stabilized by a hydrogen bond as shown in Figure 2B, is the true inhibitor, and this could mimic the “effective leaving group” of the reaction. The proposed interactions would explain the apparently inherent coupling of bond-breaking and bond-forming steps seen in reactions catalyzed by *ScTPase* and other retaining glycosyltransferases. By contrast, they are *compatible* with but not clearly *required* for glucosyl transfer via a covalent intermediate.

The available biochemical evidence for the wild-type enzyme [10, 14-16] strongly promotes studies of the *ScTPase* catalytic mechanism with site-directed mutagenesis. To provide the required structural basis, we report here on the isolation of the cDNA encoding

ScTPase and the efficient heterologous expression thereof in *E. coli*, as well as the detailed characterization of the purified recombinant enzyme. Results of secondary and threedimensional structure-based sequence comparisons and the analysis of kinetic consequences in four point mutants of *ScTPase* suggest a putative active site of the enzyme which shares striking similarity with the proposed catalytic centres of retaining GT-B fold glycosyltransferases.

EXPERIMENTAL

Materials

Validoxylamine A [17] was a kind gift from Dr. Naoki Asano (Hokuriku University, Japan). Its structure is shown in Figure 3 along with other structures discussed later. Unless otherwise mentioned all materials used have been described elsewhere [10, 14].

Molecular cloning of full-length *ScTPase*

Washed mycelia of *S. commune* BT 2115 (prepared by using reported conditions [14]) were frozen in liquid nitrogen. Total RNA was isolated from the powdered biomass using RNeasy Plant Mini kit (Qiagen). The cDNA of *S. commune* was constructed with a reverse transcription system from Promega. A pair of degenerated primers (5'-primer: 5'-GCS TTC ATY GAT GAC CKC AGA TG-3'; 3'-primer: 5'-GTC GAT SAC GTT SGG GAT RCC-3', where K = T + G, R = A + G, S = C + G, Y = C + T) were deduced from two peptides that are well conserved in fungal trehalose phosphorylases: A₃₇₁FIDDPQM₃₇₈ and G₅₀₉IPNVID₅₁₅. (The amino acid numbering of trehalose phosphorylase from *Grifola frondosa* (acc. no. BAA31350) is used [18]). A \approx 450-bp PCR product was obtained using *Taq* DNA polymerase under optimized conditions (see Supplementary Table 1), cloned into a pGEM-T-vector (Promega) and sequenced. The 5'- and 3'-end of the cDNA, containing the full-length gene encoding *ScTPase*, were obtained using GeneRacerTM kit (Invitrogen) with two pairs of

oligonucleotide primers (1: GeneRacer™ 5'-nested primer and gene-specific 3'-primer (5'-GGG GAG CTC AGG CCG GAC TTT CTT-3'); 2: gene-specific 5'-primer (5'-CCG AAC CGC GAG TAC TGC ATC CAG AT-3') and GeneRacer™ 3'-nested primer). The PCR products obtained by amplification with *Taq* DNA polymerase (see Supplementary Table 1) were cloned into a pCR 4-TOPO vector (Invitrogen) and sequenced. Amino acid sequence analysis was performed with the programmes Vector NTI (Suite 8, Informax) and SeqMan (DNASTAR).

For expression cloning, the *ScTPase* gene was amplified from the cDNA with proofreading *Pfu* DNA polymerase using two gene-specific primers (5'-primer: 5'-AGC GGA TCC TCT CCT CCC CAC GGA TTC ATG-3'; 3'-primer: 5'-ACC CTG CAG CTA GTC CTG CAC CTT GAT ACC-3', where *Bam*HI and *Pst*I restriction sites are underlined respectively). The obtained 2229-bp fragment (see Supplementary Table 1 for conditions) was digested and placed into a pQE 30 vector (Qiagen). The expression vector (pQE 30-*ScTPase*) was transferred into *E. coli* DH10B cells and the cloned insert was sequenced. Recombinant *ScTPase* contains an N-terminal fusion peptide with the sequence RGSHHHHHHGS.

Production and purification of recombinant *ScTPase*

Cells of *E. coli* DH10B harbouring pQE 30-*ScTPase* were grown in baffled 1-litre shaken flasks (37 °C; 120 rpm) containing 250 ml Luria-Bertani media supplemented with 115 mg/l ampicillin. Gene expression was induced with 0.1 mM isopropyl- β -D-thiogalactopyranoside when the culture had reached an optical density of 0.8-1.0 and continued for 18 h at 25 °C. Harvested cells were disrupted with an Aminco French press using a FA-030 cell (SLM instruments) at approximately 150 bar. After removal of cell debris at 80,000 g and 4 °C, the supernatant (\approx 15 ml containing 450 mg protein) was applied on to a XK 26/40 column packed with 50 ml of Macro-Prep DEAE Support gel (Bio-Rad) and equilibrated with 50 mM potassium phosphate buffer, pH 7.0. (Note that isolation of the His-tagged *ScTPase* using

immobilized copper affinity chromatography on a XK 16/20 Chelating Sepharose Fast Flow column was not successful because the enzyme lost most of its activity during elution with imidazole). Proteins were eluted from the anion exchange column with a linear gradient from 0-250 mM NaCl, followed by a step gradient at 500 mM and 1000 mM NaCl in the same phosphate buffer. *ScTPase* eluted at 160 mM NaCl. After change of buffer to 5 mM potassium phosphate, pH 7.0, using a HiPrep 26/10 Desalting column (GE Healthcare Bio-Sciences), the concentrated *ScTPase*-containing fractions (2.7 mg/ml) were loaded on to a XK 16/20 column packed with 22 ml of Hydroxylapatite High Resolution resin (Merck). Proteins were eluted with a linear gradient from 5-150 mM potassium phosphate, followed by a final washing step at 500 mM phosphate. *ScTPase* eluted at \approx 40 mM phosphate. Pooled fractions containing phosphorylase activity were concentrated to \approx 3 mg/ml using 10-kDa cut-off ultrafiltration concentrator tubes (Vivascience) in 50 mM potassium phosphate buffer pH 7.0 and stored at -21 °C. Protein concentration was determined using the Bio-Rad dye-binding method with BSA as the standard. Purification was monitored by SDS-PAGE, performed with a PhastSystem (GE Healthcare Bio-Sciences) using precast gradient gels (PhastGel 8-25), as well as determination of specific enzyme activity. Before further use, the enzyme storage solution was gel-filtered using a combination of NAP-5 and NAP-10 columns (GE Healthcare Bio-Sciences), equilibrated with 50 mM MES buffer, pH 6.6.

Biochemical characterization of recombinant *ScTPase*

The continuous coupled-enzyme assay of *ScTPase* activity was described elsewhere [14]. Initial rates of α,α -trehalose phosphorolysis and synthesis were recorded using discontinuous assays as reported in earlier works [10, 14] where the formation of α -D-Glc 1-P and phosphate is measured, respectively. Inhibitor binding studies were performed by using protocols developed with the native *ScTPase* [10]. Data processing for the calculation of kinetic parameters and inhibitor binding constants used reported procedures [10] (see the

Results). Molecular mass determination of *Sc*TPase by gel filtration analysis was carried out with a Superdex 200 10/300 GL High Performance column (GE Healthcare Bio-Sciences) that was equilibrated with 50 mM potassium phosphate buffer, pH 7.0, containing 150 mM sodium chloride and calibrated with Bio-Rad Gel Filtration Standard.

Analysis of alternative reactions catalyzed by *Sc*TPase

Enzymatic assays were performed in which the hydrolysis of α,α -trehalose (400 mM) or α -D-Glc 1-P (25 mM) by *Sc*TPase was measured. The enzyme (\approx 0.3 mg/ml) was incubated in the presence of substrate at 30 °C in 50 mM MES buffer, pH 6.6, and the release of glucose or phosphate was monitored over time, up to 30 h. UDP-Glc (UDP- α -D-glucose; 25 mM) was tested as a substrate of *Sc*TPase in place of α -D-Glc 1-P, whereby the time-dependent formation of UDP was recorded in the absence or presence of glucose (400 mM) under the conditions described above. The UDP concentration in samples taken from the reaction mixture was determined enzymatically [19]. Appropriate controls lacking *Sc*TPase were always recorded, and the reported values are corrected for blank readings which were typically < 10% of the enzymatic rates.

Characterization of recombinant *Sc*TPase by MS

Metal analysis was performed with inductively coupled plasma MS, as previously published [10]. Protein and peptide MS was performed on a Q-TOF Ultima Global (Waters Micromass) mass spectrometer equipped with a standard electrospray unit, a Cap-LC System (Waters Micromass) and a 10-port solvent switch module (Rheodyne). Approx. 200 – 300 pmol of protein were loaded onto a BioBasic C4 column (Thermo Electron) and eluted with an increasing gradient of acetonitrile. 5 μ g of protein were subjected to SDS-PAGE, destained, carbamidomethylated, digested with trypsin and extracted from gel pieces as described elsewhere [20]. Dried extracts were reconstituted in 0.1% formic acid before LC ESI Q-TOF MS analysis. Peptides were captured on an Aquasil C18 precolumn (Thermo Electron) before

elution from the analytical column with a linear gradient from 5 to 50% of acetonitrile. Samples were analyzed in the MS and tandem MS mode and data analysis was performed with MassLynx 4.0 SP4 and BioLynx Software (Waters Micromass).

Site-directed mutagenesis

Site-directed mutations were introduced with a Two-Stage PCR protocol [21], employing pQE 30-*ScTPase* as the template. In the first step, two separate primer extension reactions were performed using the forward oligonucleotide primer and its reverse complementary, respectively. The following mutation primers were used where the mismatched parts are underlined: D379N, 5'-GCA TTC ATT GAC AAC CCG CAG ATG C-3'; H403A, 5'-AC CGC TCG GCC ATT GAG ATC AGG-3'; R507A, 5'-GC ATC CAG ATC GCG GCG TTC GAC CCG G-3'; K512A, 5'-C GAC CCG GCG GCG GGC ATC CCG AAC G-3'. In the second step, the two reactions were combined and amplification was continued (see Supplementary Table 1 for detailed PCR conditions). After digestion of the template DNA with *DpnI*, the amplified plasmid vectors were transformed into electro-competent cells of *E. coli* JM109. Plasmid miniprep DNA from positive clones was subjected to dideoxy sequencing of the entire *ScTPase* gene to verify that the desired mutation had been introduced and no base misincorporations had occurred because of DNA polymerase errors. Expression and purification of *ScTPase* mutants were carried out as described above.

RESULTS

Gene cloning, and heterologous expression and purification of recombinant *ScTPase*

The cDNA encoding the full-length *ScTPase* was isolated, cloned and sequenced. The entire open reading frame consists of 2247 bp, including the codon for the initiator methionine and the stop-codon. The recombinant *ScTPase* is a protein of 748 amino acids (including the tag of 11 extra amino acids at its N-terminus) with a calculated molecular mass of 82,803 Da. An

alignment of the primary structures (see Supplementary Figure 1) shows that *ScTPase* (acc. no. DQ357198) is 76.7% and 73.0% identical to fungal trehalose phosphorylases from *G. frondosa* (acc. no. BAA31350) [18] and *Pleurotus sajor-caju* (acc. no. AAF22230) [22], respectively. Screening of the non-redundant protein sequence data base with the amino acid sequence of *ScTPase* confirmed the proposed membership [10] of the enzyme to family GT-4 glycosyltransferases (data not shown). Interestingly, the C-terminal part of *ScTPase* is 20.2% identical to trehalose synthase, a 416 amino acid GT-4 glycosyltransferase from the archaeon *Pyrococcus horikoshii* (acc. no. BAA30133) [23]. The trehalose synthase appears to be a truncated homologue of *ScTPase*, lacking entirely the \approx 330 amino acid-long N-terminal domain of the fungal enzyme.

The specific *ScTPase* activity of the induced *E. coli* cell extract was 0.7 U/mg and can be compared with a value of 0.06 U/mg found in *S. commune* [14]. Highly purified recombinant *ScTPase* shows a specific activity of 6.3 U/mg. It was obtained in a yield of 32% by using an optimized protocol, where an anion exchange and a hydroxylapatite chromatographic step were employed sequentially. (A detailed summary of the purification is available in Supplementary Table 2). Stabilizers such as glycerol or α,α -trehalose that were required to prevent inactivation of the natural enzyme [14] were not needed during isolation and storage (at -21 °C) of the recombinant *ScTPase*.

Structural properties of recombinant *ScTPase*

Recombinant *ScTPase* shows a molecular mass of \approx 80 kDa (Figure 4B), in good agreement with the predicted mass of the full-length protein. The purified enzyme eluted from a Superdex size exclusion column as shown in Figure 4A where the main protein peak corresponded to a 165-kDa dimer and contained about 60% of the total protein and 85% of the total activity. A minor fraction, eluting as a distinct shoulder of the main peak, accounted for the remainder protein and activity, and corresponded to a 81-kDa monomer. The specific

activity of the 81-kDa fraction (1.6 U/mg) was only $\frac{1}{4}$ that of the major form. Using non-denaturing anionic PAGE, the co-existence of dimer and monomeric forms in the recombinant enzyme was confirmed (Figure 4A, inset). Analysis by inductively coupled plasma MS showed that recombinant *ScTPase* contained less than 0.01 g-atom Mg^{2+} per protein monomer, in marked contrast to the natural enzyme isolated from *S. commune* in which each monomer had a g-atom equivalent of Mg^{2+} bound in non-dissociable manner [10].

Upon storage at 4 °C (50 mM potassium phosphate buffer, pH 7.0), we observed a defined and highly reproducible conversion of the recombinant *ScTPase* into two fragments of ≈ 65 kDa and ≈ 16 kDa molecular mass (Figure 4B). After clear-cut separation of the two protein forms by gel filtration, the 65-kDa fragment (61 005 Da by LC ESI Q-TOF MS) was found to have the same specific activity as the full-length precursor protein (6 U/mg) whereas the 16-kDa protein was completely inactive. The truncated *ScTPase* eluted from the size exclusion column in a single fraction corresponding to a 125-kDa dimer. Interestingly, natural *ScTPase* was isolated from the fungus as a shortened protein variant of a similar mass of ≈ 61 kDa but was monomeric [14]. Peptide mass fingerprints of the tryptic digests of full-length *ScTPase* and the two fragments derived from it are reported in Table 1. It is not known whether polypeptide chain cleavage in *ScTPase* is autocatalytic, uncatalyzed, or results from a minor contamination with protease not detectable at the protein level. Our attempts to produce in *E. coli* a truncated version of recombinant *ScTPase* (1644 bp; residues Asn-189 to Asp-737) containing or lacking an N-terminal His-tag failed due to excessive formation of protein inclusion bodies, even at low growth temperatures of 15 °C. The proteolytic conversion of *ScTPase* was not further pursued, in particular because it does not affect the enzyme activity.

Kinetic properties and inhibition of recombinant *ScTPase*

Kinetic parameters of full-length *ScTPase* are summarized in Table 2 along with the corresponding parameters of the truncated enzyme isolated from *S. commune* which have

been reported [10]. Catalytic centre activities (k_{cat}) as well as binding (K_i) and Michaelis constants (K_m) for the substrates were very similar for both phosphorylase forms. The results imply that the enzymatic reaction co-ordinate, at the points defined by Figure 2A, is not significantly altered by the N-terminal truncation of the intact enzyme. Table 2 also shows inhibition constants (K_{ic}) for the proposed transition-state analogue vanadate in combination with glucose (see Figure 2B) or α,α -trehalose. The K_{ic} values were almost identical for the two enzymes.

The pseudodisaccharide validoxylamine A (Figure 3) is a potent inhibitor of *Sc*TPase, acting competitively against α,α -trehalose with a K_i value of $1.7 (\pm 0.2)$ μM . It binds about 350-fold more tightly to the enzyme-phosphate complex than α,α -thio-trehalose [10], a close structural analogue of α,α -trehalose (see Figure 3) that is not phosphorolysed by the enzyme and can probably mimic disaccharide substrate binding in the ground state.

*Sc*TPase, intact or truncated, displays a very weak but significant hydrolytic activity towards α,α -trehalose and α -D-Glc 1-P in the absence of phosphate and glucose, respectively. The disaccharide (400 mM) and α -D-Glc 1-P (25 mM) were converted at approx. 0.002% (\pm 0.0003%) of the corresponding phosphorolysis and synthesis rate recorded under otherwise identical conditions in the presence of 50 mM phosphate and 400 mM glucose, respectively. The limited availability of purified natural enzyme precluded detection of this low activity in our previous studies of *Sc*TPase [10, 14]. The result is interesting because it shows that occupancy of the phosphate site and sugar binding subsite +1 is not an absolute requirement for glucosyl transfer to occur, even though the minute "error" reaction with water is not a relevant component of the normal catalytic pathway.

Incubation of *Sc*TPase with UDP-Glc (25 mM) in the presence or absence of glucose (400 mM) did not yield UDP within limits of detection by the enzymatic assay (\approx 0.001% of k_{cat} for synthesis). UDP-Glc, however, acts as competitive inhibitor against phosphate and α -

D-Glc 1-P as well as against α,α -trehalose when the phosphate concentration is non-saturating. A K_{ic} of ≈ 12 mM has been determined using initial rates measured in phosphorolysis direction at a constant concentration of α,α -trehalose (100 mM) and a varied concentration of phosphate. Phosphorylase inhibition by UDP-Glc, recorded at constant and non-saturating substrate levels of 5 mM phosphate and 100 mM α,α -trehalose, increased only marginally (< 1.5 -fold) in response to an increase in the glucose concentration from K_m (50 mM) to a saturating level (400 mM), indicating that formation of an abortive ternary complex does not occur.

Sequence analysis and site-directed mutagenesis

A pairwise alignment of the primary structures of *Sc*TPase and maltodextrin phosphorylase from *E. coli* (*Ec*MalP), a well-characterized α -retaining glucosyltransferase of family GT-35 [12, 24-26], revealed that in spite of the low overall sequence identity of 11.6%, the catalytic residues of *Ec*MalP appear to be highly conserved in *Sc*TPase. Recent X-ray structures of enzyme members of families GT-5 (glycogen synthase) [27, 28], GT-20 (trehalose 6-phosphate synthase) [29, 30], and GT-72 (AGT, α -glucosyltransferase) [31] support a distinct pattern of active site conservation among clan IV glycosyltransferases of fold family GT-B. Figure 5 shows a partial multiple sequence alignment in which the known catalytic centre residues were used to identify their likely functional homologues in *Sc*TPase and thus select candidates for site-directed mutagenesis. (The full alignment is found in Supplementary Figure 2.) Glu-606 and Glu-614 of *Sc*TPase comprise the so-called GPGT (glycogen phosphorylase glycosyltransferase) superfamily motif ("EX₇E" where X is any amino acid), originally identified in the sequence work of Wrabl and Grischin [32], whereby Glu-606 may be replaced by an aspartate (family GT-20 [29]) and Glu-614 by a histidine, tyrosine or phenylalanine (family GT-5 [27, 33]). Furthermore, Glu-614 is replaced by the pyridoxal 5'-phosphate-binding lysine in family GT-35 [24]. Results of mutagenesis experiments with

different glycosyltransferases [34, 35], among them the α -mannosyltransferase AceA of family GT-4 [36], suggest that GPGT motif residues are essential, and the available crystal structures reveal their conserved role in positioning the glycosyl donor for catalysis in subsite -1 [12, 27, 30]. Arg-507 and Lys-512 of *ScTPase* are homologous in the sequence to key phosphate binding residues of *EcMalP* [12, 24] as well as of *E. coli* trehalose 6-phosphate synthase OtsA [29, 30]. Their exact function in enzymes of family GT-4 is not well defined, except for the reported complete loss of activity in Lys-into-Ala variant of AceA [36]. The motif Gly²⁹¹-Gly-Val²⁹³ of *ScTPase* corresponds to similar motifs in *EcMalP* (Gly¹¹⁴-Gly-Leu¹¹⁶) and OtsA (Gly²²-Gly-Leu²⁴), whereby the main chain NH of the second glycine interacts with an oxygen of the substrate phosphate in *EcMalP* and the β -phosphate group of the UDP leaving group in OtsA. Comparison of the known secondary structure compositions of *EcMalP* and OtsA to that predicted for *ScTPase* suggests that Asp-379 and His-403 are homologous to Asp-308 and His-348 of *EcMalP* (Figure 5). Both residues are important for the activity of *EcMalP*. Asp-308 seems to position the substrate for catalysis through strong hydrogen bonding interactions with the leaving group at sugar-binding subsite +1 [12 and refs. therein]. His-348 is thought to stabilize the glucosyl oxocarbenium ion-like transition at the catalytic subsite -1 [12, 37].

By site-directed mutagenesis, *ScTPase* residues Asp-379, His-403, Arg-507 and Lys-512 were individually replaced with an alanine. Because the D379A mutant could not be produced as a soluble recombinant protein in *E. coli*, Asp-379 was alternatively substituted by an asparagine. Each *ScTPase* mutant was prepared by using procedures exactly as described for the wild-type. A SDS polyacrylamide gel displaying the purified point mutants along with the wild-type is shown in Figure 6. Initial-rate measurements performed in the direction of phosphorolysis of α,α -trehalose under conditions of apparent substrate saturation of the wild-type (400 mM α,α -trehalose; 50 mM phosphate) revealed that each site-directed replacement

had introduced a large, between $10^{3.2}$ to $10^{5.6}$ -fold catalytic defect in the corresponding *ScTPase* variant. The R507A mutant was also assayed for its ability to catalyze the synthesis of α,α -trehalose (50 mM α -D-Glc 1-P; 400 mM glucose), and the activity loss in the mutant in comparison with the wild-type was comparable in each direction of the reaction. The hydrolase activity of each mutant was determined in the absence of phosphate using 400 mM α,α -trehalose as the substrate and in marked contrast to the phosphorylase activity, it was similar or even increased in the mutants, compared with the wild-type activity. The ratio of apparent catalytic rates of phosphorolysis and hydrolysis of α,α -trehalose thus decreased by a factor of up to 10^6 from a value of $4.6 \cdot 10^4$ in the wild-type to $7.8 \cdot 10^{-2}$ in R507A. Three *ScTPase* mutants (D379N, R507A and K512A) were "better" hydrolases than phosphorylases under the conditions used. The results are summarized in Table 3.

DISCUSSION

Structure-function relationships for *ScTPase* and related family GT-4 glycosyltransferases

Family GT-4 is the presently second largest glycosyltransferase family [1, 3]. Its members are from all three domains of life and represent a wide range of donor and acceptor substrate specificities. However, little is known about structure-function relationships and the mechanism of family GT-4 enzymes. The reaction catalysed by trehalose phosphorylase is unique among those reported for family GT-4 glycosyltransferases and appears to be particularly conducive to mechanistic studies. It is freely reversible *in vitro*, and reactants and products have relatively simple chemical structures for which site-specifically modified analogues are readily accessible [10, 25, 32]. Point mutants of recombinant *ScTPase* can now also be generated as particular probes of mechanism.

Lacking a three-dimensional structure of a GT-4 glycosyltransferase, identification of candidate residues of *ScTPase* for site-directed replacement has relied on comparison with

template structures, using retaining glycosyltransferases of fold family GT-B. Results summarized in Figure 5 suggest close similarity in active site topology between *ScTPase* and enzymes of families GT-5, GT-20, and GT-35. Analysis of kinetic consequences in *ScTPase* mutants revealed that residues pinpointed by a clear conservation pattern (Asp-379, His-403, Arg-507 and Lys-512 in addition to GPGT motif residues) are clearly important for the activity of *ScTPase*.

The results also advance, on a more global level than Figure 5, the structure-function relationships of *ScTPase*. The molecular sizes of family GT-4 proteins vary in the approximate range of ≈ 300 to ≈ 1100 amino acids, hence *ScTPase* with its 737 residues is among the large members. The highly purified enzyme is readily converted into a 65-kDa short-form variant which probably explains why only the truncated *ScTPase* could be isolated from *S. commune* [14]. Cleavage of the full-length phosphorylase appears to occur predominantly between residues Asn-189 and Gly-188 (Table 1) and does not impact significantly on activity and stability. The results do not support an immediate correlation between N-terminal truncation and protein monomerisation and Mg^{2+} binding which are properties of the natural ≈ 61 -kDa enzyme [10, 14] that are lacking in the recombinant counterpart. However, the kinetic parameters described imply that the crucial elements of catalytic function of *ScTPase* reside completely in the C-terminal protein part.

Family GT-4 comprises glycosyltransferases with different specificities for the leaving group of their respective glycosyl donor substrate. It is interesting therefore that *ScTPase* binds UDP-Glc although it is unable to utilize the nucleotide sugar as an alternative substrate for the enzymatic reaction with glucose or water, respectively. Binding studies reveal that sugar binding subsite -1 and the phosphate site are both occupied in the enzyme-UDP-Glc complex. The binding affinity of UDP-Glc ($K_{ic} \approx 12$ mM) is comparable to that of α -D-Glc 1-P ($K_i = 6$ mM; Table 2) but 3 - 4 orders of magnitude smaller than the typical affinities of

nucleotide sugar-dependent glycosyltransferases for their donor substrates [34, 38]. The absence of detectable transferase activity with UDP-Glc is most simply explained by its non-productive binding to *ScTPase*. Another possibility suggested by the results is, however, that bound UDP-Glc does not promote glucose binding at subsite +1, perhaps because steric conflicts occur in a ternary complex or the required binding recognition of glucose is not induced. One of closest enzyme homologues of *ScTPase* that has been characterized is the UDP-Glc-dependent trehalose synthase from the archaeon *P. horikoshii* which is not active as a phosphorylase [23]. We therefore performed a structure-based sequence comparison of *ScTPase* and *P. horikoshii* trehalose synthase using *EcMalP* and *OtsA* as templates of phospho-sugar and nucleotide-sugar-dependent glycosyltransferases, respectively. The analysis did not pinpoint candidate residues determining the "phosphorylase to synthase" switch in α,α -trehalose-metabolising enzymes of family GT-4.

Implications for the catalytic mechanism

Figure 5 suggests that *ScTPase* probably shares salient features of the catalytic mechanism with other retaining glycosyltransferases of fold family GT-B. Residues contributed to the phosphate site (Arg-507 and Lys-512) and sugar subsite +1 (Asp-379) of *ScTPase* are of particular interest as they seem to determine the exquisite selectivity of the wild-type enzyme for the phosphorolysis compared with the hydrolysis of α,α -trehalose. Individual substitutions of Asp-379, Arg-507 and Lys-512 nearly reversed the original selectivity of the enzyme such that hydrolysis of the glucosyl donor substrate was now preferred, up to 100-fold, in the respective site-directed mutant. Considering Figures 2B and 5, the three conserved residues are also relevant with respect to the transition state-like inhibition of *ScTPase* by vanadate in combination with glucose [15], and a systematic dissection of this two-component inhibitor could now be possible by using mutagenesis. If *ScTPase* utilized the catalytic mechanism

shown in Figure 1, Asp-379, Arg-507 and Lys-512 might also be crucial to promote the initial attack of phosphate on the glycosidic bond of α,α -trehalose.

Validoxylamine A is the most powerful inhibitor of *Sc*TPase presently known. We see its particular prowess as a mechanistic probe for the enzyme in the fact that it provides partial analogy to the proposed glucosyl oxocarbenium ion-like transition state of the reaction, particularly with regard to the build-up of positive charge at the substituted anomeric carbon [for a discussion, see 14]; and that upon binding to the enzyme-phosphate complex, it mimics the catalytically critical ternary complex which the previously examined iminosugars 1-deoxynojirimycin and isofagomine (Figure 3; [15]) could not. It was shown in earlier studies of α -glucosyl hydrolases that the inhibitory properties of N-linked pseudo-disaccharides are dependent upon the whole unit and not the individual constituent parts [17, 39, 40]. The very high affinity of validoxylamine A for binding to pig kidney trehalase ($K_i = 0.52$ nM) derives from the synergistic interaction of its two cyclitol units with enzyme subsites -1 and +1 [17, 39]. Strong inhibition of amylolytic enzymes by the pseudo-tetrasaccharide acarbose requires that the acarviosine moiety, as shown in Figure 3, is intact [40]. There is overlap in binding recognition of subsites -1 and +1 in *Sc*TPase [15, 16] and therefore the orientation of validoxylamine A in the active centre is not unambiguously defined. The conformation of the hydroxymethylconduritol unit of the inhibitor is constrained by the double bond between C5 and C7 (which corresponds to the endocyclic O5 in glucose) to a 2H_3 half-chair in which atoms C4, C5, C7 and C1 are coplanar (Figure 3). Atoms C2 and C3 are above and below the plane, respectively. This conformation is clearly not an ideal mimic of the glucosyl oxocarbenium ion-like transition state which is expected to be constrained to a 4H_3 half-chair or a sofa conformation because of the partial double bond between C1 and O5 that leads to coplanarity of the atoms C5, O5, C1 and C2. In the endocyclic enitol D-glucal (Figure 3) the atoms O5, C1, C2 and C3 are coplanar, and this compound binds well to subsite +1 ($K_i = 0.32$

mM [10]), in spite of the fact that the sp^2 -hybridized C1 would be a clear feature of a good transition state mimic, which should bind selectively to subsite -1. Therefore, reversal of the anticipated binding mode of the pseudo-disaccharide in which the hydroxymethylconduritol group would be positioned in the catalytic subsite -1 cannot be discounted. Nevertheless, despite the lack of good complementarity with the proposed transition state structure and the perhaps incomplete subsite selectivity of validoxylamine A, the observed high affinity is interesting because it suggests that the inhibitor may exploit electrostatic interactions between its (positively charged) amino group and enzyme-bound phosphate for binding. In the S_Ni -like mechanism, the electrostatic "front-side" stabilisation of the oxocarbenium ion-like transition state by the attacking anionic nucleophile is thought to be a crucial catalytic factor [4].

ACKNOWLEDGEMENTS

Financial support from the Austrian Science Funds FWF (P15118-B09; PhD programme "Molecular Enzymology") is gratefully acknowledged. We thank Prof. Friedrich Altmann and Dr. Daniel Kolarich (Department of Chemistry, University of Applied Life Sciences and Natural Resources, Vienna) for MS analysis; and Prof. Dr. Naoki Asano (Hokuriku University, Japan) for the generous gift of validoxylamine A.

REFERENCES

- 1 Davies, G. J., Gloster, T. M. and Henrissat, B. (2005) Recent structural insights into the expanding world of carbohydrate-active enzymes. *Curr. Opin. Struct. Biol.* **15**, 637-645
- 2 Breton, C., Snajdrova, L., Jeanneau, C., Koca, J. and Imberty, A. (2006) Structures and mechanisms of glycosyltransferases. *Glycobiology* **16**, 29-37
- 3 Coutinho, P. M., Deleury, E., Davies, G. J. and Henrissat, B. (2003) An evolving hierarchical family classification for glycosyltransferases. *J. Mol. Biol.* **328**, 307-317
see also: <http://www.cazy.org/CAZY/>
- 4 Davies, G. J., Sinnott, M. L. and Withers, S. G. (1998) Glycosyl transfer. In *Comprehensive Biological Catalysis* (Sinnott, M. L., ed.), pp. 119-208, Academic press, San Diego
- 5 Lairson, L. L. and Withers, S. G. (2004) Mechanistic analogies amongst carbohydrate modifying enzymes. *Chem. Commun.* **20**, 2243-2248
- 6 Zechel, D. L. and Withers, S. G. (2000) Glycosidase mechanisms: anatomy of a finely tuned catalyst. *Acc. Chem. Res.* **33**, 11-18
- 7 Vasella, A., Davies, G. J. and Bohm, M. (2002) Glycosidase mechanisms. *Curr. Opin. Chem. Biol.* **6**, 619-629
- 8 Mosi, R. and Withers, S. G. (1999) Synthesis and kinetic evaluation of 4-deoxymaltopentaose and 4-deoxymaltohexaose as inhibitors of muscle and potato α -glucan phosphorylases. *Biochem. J.* **338**, 251-256
- 9 Ly, H. D., Loughheed, B., Wakarchuk, W. W. and Withers, S. G. (2002) Mechanistic studies of a retaining α -galactosyltransferase from *Neisseria meningitidis*. *Biochemistry* **41**, 5075-5085
- 10 Eis, C., Watkins, M., Prohaska, T. and Nidetzky, B. (2001) Fungal trehalose phosphorylase: kinetic mechanism, pH-dependence of the reaction and some structural properties of the enzyme from *Schizophyllum commune*. *Biochem. J.* **356**, 757-767
- 11 Persson, K., Ly, H. D., Dieckelmann, M., Wakarchuk, W. W., Withers, S. G. and Strynadka, N. C. (2001) Crystal structure of the retaining galactosyltransferase LgtC from *Neisseria meningitidis* in complex with donor and acceptor sugar analogs. *Nat. Struct. Biol.* **8**, 166-175

- 12 Watson, K. A., McCleverty, C., Geremia, S., Cottaz, S., Driguez, H. and Johnson, L. N. (1999) Phosphorylase recognition and phosphorolysis of its oligosaccharide substrate: answers to a long outstanding question. *EMBO J.* **18**, 4619-4632
- 13 Sinnott, M. L. and Jencks, W. P. (1980) Solvolysis of D-glucopyranosyl derivatives in mixtures of ethanol and 2,2,2-trifluoroethanol. *J. Am. Chem. Soc.* **102**, 2026-2032
- 14 Eis, C. and Nidetzky, B. (1999) Characterization of trehalose phosphorylase from *Schizophyllum commune*. *Biochem. J.* **341**, 385-393
- 15 Nidetzky, B. and Eis, C. (2001) α -Retaining glucosyl transfer catalysed by trehalose phosphorylase from *Schizophyllum commune*: mechanistic evidence obtained from steady-state kinetic studies with substrate analogues and inhibitors. *Biochem. J.* **360**, 727-736
- 16 Eis, C. and Nidetzky, B. (2002) Substrate-binding recognition and specificity of trehalose phosphorylase from *Schizophyllum commune* examined in steady-state kinetic studies with deoxy and deoxyfluoro substrate analogues and inhibitors. *Biochem. J.* **363**, 335-340
- 17 Asano, N. (2003) Glycosidase inhibitors: update and perspectives on practical use. *Glycobiology* **13**, 93-104
- 18 Saito, K., Yamazaki, H., Ohnishi, Y., Fujimoto, S., Takahashi, E. and Horinouchi, S. (1998) Production of trehalose synthase from a basidiomycete, *Grifola frondosa*, in *Escherichia coli*. *Appl. Microbiol. Biotechnol.* **50**, 193-198
- 19 Fujii, H. and Miwa, S. (1983) Pyruvate kinase. In *Methods of Enzymatic Analysis* (Bergmeyer, H. U., ed.), pp. 496-507, Verlag Chemie, Weinheim
- 20 Kolarich, D. and Altmann, F. (2000) N-Glycan analysis by matrix-assisted laser desorption/ionization mass spectrometry of electrophoretically separated nonmammalian proteins: application to peanut allergen Ara h 1 and olive pollen allergen Ole e 1. *Anal. Biochem.* **285**, 64-75
- 21 Wang, W. and Malcolm, B. A. (1999) Two-stage PCR protocol allowing introduction of multiple mutations, deletions and insertions using QuikChange Site-Directed Mutagenesis. *Biotechniques* **26**, 680-682
- 22 Han, S. E., Kwon, H. B., Lee, S. B., Yi, B. Y., Murayama, I., Kitamoto, Y. and Byun, M. O. (2003) Cloning and characterization of a gene encoding trehalose phosphorylase (TP) from *Pleurotus sajor-caju*. *Protein Expr. Purif.* **30**, 194-202

- 23 Ryu, S. I., Park, C. S., Cha, J., Woo, E. J. and Lee, S. B. (2005) A novel trehalose-synthesizing glycosyltransferase from *Pyrococcus horikoshii*: molecular cloning and characterization. *Biochem. Biophys. Res. Commun.* **329**, 429-436
- 24 Watson, K. A., Schinzel, R., Palm, D. and Johnson, L. N. (1997) The crystal structure of *Escherichia coli* maltodextrin phosphorylase provides an explanation for the activity without control in this basic archetype of a phosphorylase. *EMBO J.* **16**, 1-14
- 25 O'Reilly, M., Watson, K. A. and Johnson, L. N. (1999) The crystal structure of the *Escherichia coli* maltodextrin phosphorylase-acarbose complex. *Biochemistry* **38**, 5337-5345
- 26 Geremia, S., Campagnolo, M., Schinzel, R. and Johnson, L. N. (2002) Enzymatic catalysis in crystals of *Escherichia coli* maltodextrin phosphorylase. *J. Mol. Biol.* **322**, 413-423
- 27 Buschiazzo, A., Ugalde, J. E., Guerin, M. E., Shepard, W., Ugalde, R. A. and Alzari, P. M. (2004) Crystal structure of glycogen synthase: homologous enzymes catalyze glycogen synthesis and degradation. *EMBO J.* **23**, 3196-3205
- 28 Horcajada, C., Guinovart, J. J., Fita, I. and Ferrer, J. C. (2006) Crystal structure of an archaeal glycogen synthase: insights into oligomerization and substrate binding of eukaryotic glycogen synthases. *J. Biol. Chem.* **281**, 2923-2931
- 29 Gibson, R. P., Turkenburg, J. P., Charnock, S. J., Lloyd, R. and Davies, G. J. (2002) Insights into trehalose synthesis provided by the structure of the retaining glucosyltransferase OtsA. *Chem. Biol.* **9**, 1337-1346
- 30 Gibson, R. P., Tarling, C. A., Roberts, S., Withers, S. G. and Davies, G. J. (2004) The donor subsite of trehalose-6-phosphate synthase: Binary complexes with UDP-glucose and UDP-2-deoxy-2-fluoro-glucose at 2 Å resolution. *J. Biol. Chem.* **279**, 1950-1955
- 31 Lariviere, L., Sommer, N. and Morera, S. (2005) Structural evidence of a passive base-flipping mechanism for AGT, an unusual GT-B glycosyltransferase. *J. Mol. Biol.* **352**, 139-150
- 32 Wrabl, J. O. and Grishin, N. V. (2001) Homology between O-linked GlcNAc transferases and proteins of the glycogen phosphorylase superfamily. *J. Mol. Biol.* **314**, 365-374
- 33 Yep, A., Ballicora, M. A. and Preiss, J. (2004) The active site of the *Escherichia coli* glycogen synthase is similar to the active site of retaining GT-B glycosyltransferases. *Biochem. Biophys. Res. Commun.* **316**, 960-966

- 34 Yep, A., Ballicora, M. A., Sivak, M. N. and Preiss, J. (2004) Identification and characterization of a critical region in the glycogen synthase from *Escherichia coli*. *J. Biol. Chem.* **279**, 8359-8367
- 35 Schinzel, R. and Palm, D. (1990) *Escherichia coli* maltodextrin phosphorylase: contribution of active site residues glutamate-637 and tyrosine-538 to the phosphorolytic cleavage of α -glucans. *Biochemistry* **29**, 9956-9962
- 36 Abdian, P. L., Lellouch, A. C., Gautier, C., Ielpi, L. and Geremia, R. A. (2000) Identification of essential amino acids in the bacterial α -mannosyltransferase AceA. *J. Biol. Chem.* **275**, 40568-40575
- 37 Schwarz, A., Pierfederici, F. M. and Nidetzky, B. (2005) Catalytic mechanism of α -retaining glucosyl transfer by *Corynebacterium callunae* starch phosphorylase: the role of histidine-334 examined through kinetic characterization of site-directed mutants. *Biochem. J.* **387**, 437-445
- 38 Flint, J., Taylor, E., Yang, M., Bolam, D. N., Tailford, L. E., Martinez-Fleites, C., Dodson, E. J., Davis, B. G., Gilbert, H. J. and Davies, G. J. (2005) Structural dissection and high-throughput screening of mannosylglycerate synthase. *Nat. Struct. Mol. Biol.* **12**, 608-614
- 39 Asano, N., Kato, A. and Matsui, K. (1996) Two subsites on the active center of pig kidney trehalase. *Eur. J. Biochem.* **240**, 692-698
- 40 Kim, M.-J., Lee, S.-B., Lee, H.-S., Lee, S.-Y., Baek, J.-S., Kim, D., Moon, T.-W., Robyt, J. F. and Park, K.-H. (1999) Comparative study of the inhibition of α -glucosidase, α -amylase, and cyclomaltodextrin glucanosyltransferase by acarbose, isoacarbose, and acarviosine-glucose. *Arch. Biochem. Biophys.* **371**, 277-283

FIGURE LEGENDS

Figure 1: Phosphorolysis of α,α -trehalose by a hypothetical S_Ni -like mechanism. For further explanations, see text. The reaction is thought to proceed through an oxocarbenium ion-like transition state.

Figure 2: Steady-state kinetic mechanism of *ScTPase* (A) and suggested interactions leading to the transition state-like inhibition by orthovanadate and glucose (B). In panel A, K_i is a dissociation constant.

Figure 3: Structures of common inhibitors of glycosyl hydrolases and glycosyltransferases including *ScTPase*. **A** validoxylamine A (1.7; this work); **B** α,α -thio-trehalose (560) [10]; **C** acarviosine unit of acarbose (n.a.); **D** isofagomine (56) [15]; **E** 1-deoxynojirimycin (1200) [15]; **F** D-glucal (320) [10]. Values in parentheses show inhibition constants in μM which describe binding of the inhibitor to the complex of *ScTPase* and phosphate; n.a., not applicable.

Figure 4: Structural characterization of recombinant *ScTPase* by size exclusion chromatography (A) and spontaneous truncation of the full-length enzyme during storage at 4 °C (B). The insets of panel A show (1) the molecular mass determination for *ScTPase* where the open circle and the full triangle indicate the dimeric (165 kDa) and monomeric (81 kDa) enzyme forms, respectively and full circles are the molecular mass marker proteins; and (2) the detection of dimeric and monomeric *ScTPase* by using non-denaturing anionic PAGE. In panel B, a SDS polyacrylamide gel of the purified recombinant *ScTPase* (2.5 mg/ml) is shown before and after incubation at 4 °C for ~ 340 h in 50 mM potassium phosphate buffer, pH 7.0.

Figure 5: Partial multiple alignment of primary structures of *ScTPase* and retaining glycosyltransferases of fold family GT-B (A) and hypothetical active centre of *ScTPase* derived from results of comparative sequence analysis and site-directed mutagenesis (B). In panel A are shown the regions surrounding catalytic centre residues in *EcMalP* [12] (*E. coli* maltodextrin phosphorylase; acc. no. AAC76442); *OtsA* [30] (*E. coli* trehalose 6-phosphate synthase, acc. no. AAS99849) and *AtGS* [27] (*Agrobacterium tumefaciens* glycogen synthase,

acc. no. AAL44876) and compared with the counterpart regions in *ScTPase* (acc. no. DQ357198). Also shown are the secondary structural elements (black cylinders for α -helices and arrows for β -sheets) for *EcMalP*, whereby the numbering corresponds to that of Watson *et al.* [24], aligned to the predicted secondary structural elements for *ScTPase*, numbers indicated in parenthesis. Secondary structure prediction was made with the public PSIPRED server (<http://bioinf.cs.ucl.ac.uk/psipred/>) using mGenTHREADER method. Panel B shows the hypothetical map of active-site interactions in *ScTPase* with the corresponding residues of *EcMalP* indicated in parenthesis.

Figure 6: Analysis by SDS PAGE of purified recombinant *ScTPase* and site-directed mutants thereof. Lanes 1-7: 1,7 low molecular mass standard; 2, recombinant *ScTPase*; 3, D379N; 4, H403A; 5, R507A; 6, K512A.

Figure 1

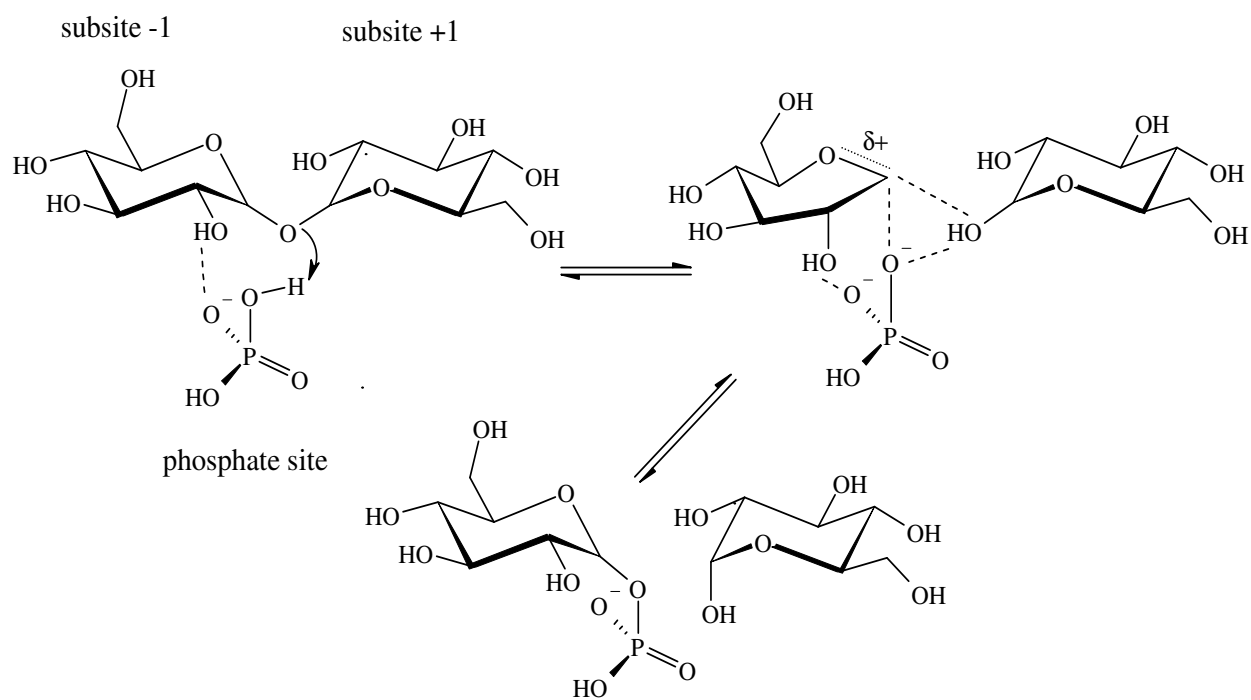


Figure 2

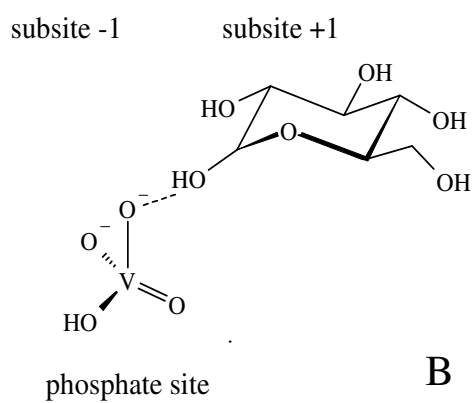
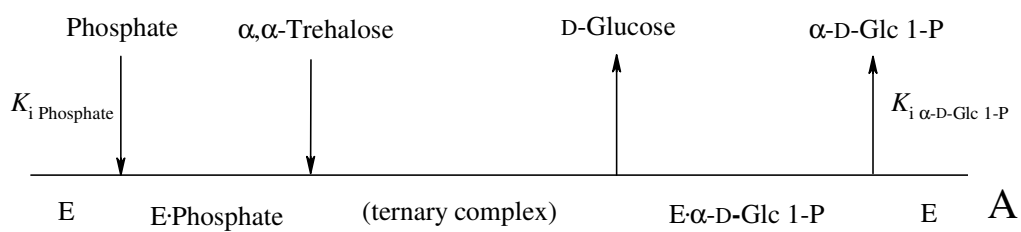


Figure 3

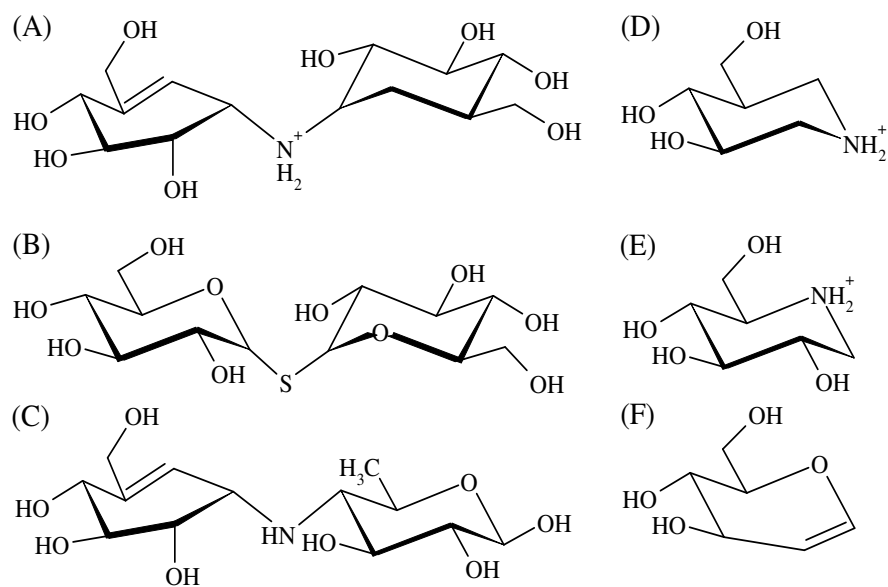
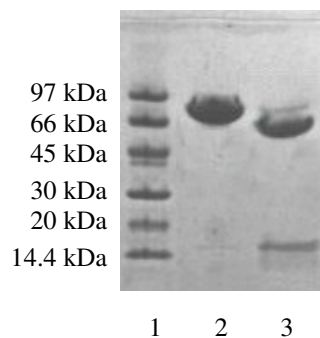
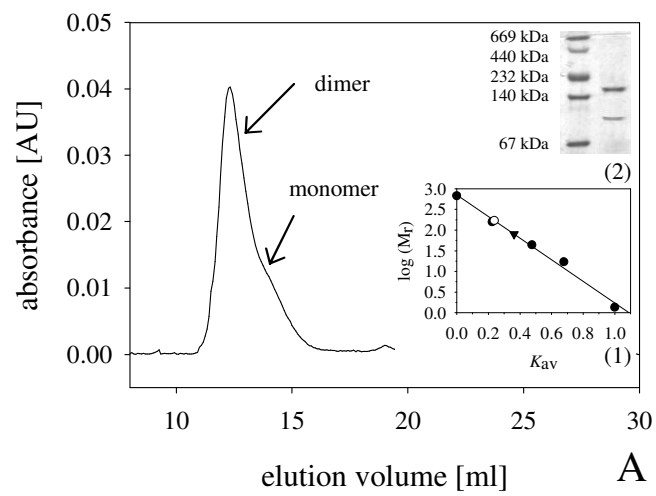


Figure 4



B

Figure 5

Enzyme	GT family	Phosphate site	Sugar subsite +1	Sugar subsite -1	Phosphate site	GPGT motif
<i>AtGS</i>	5	-IKTGG ¹⁸ LADV	MVHAHD ¹³⁸ WQAAM	SLLTIH ¹⁶³ NIAFQ	ISR ²⁹⁹ LTWQK ³⁰⁴ GID	FE ³⁷⁶ PCGLTQLY ³⁸⁴ A
<i>OtsA</i>	20	AASAGG ²³ LAVGI	IIWIHD ¹³¹ YHL-L	IGFFLH ¹⁵⁵ IP---	VER ²⁶³ LDYSK ²⁶⁸ GLP	RD ³⁶² GMNLVAK ³⁷⁰ Y
<i>EcMalP</i>	35	ALGNGG ¹¹⁵ LGRLA	VIQIND ³⁰⁸ THP-T	FAYTNH ³⁴⁶ TL---	IKR ⁵³⁵ LHEYK ⁵⁴⁰ RQH	KE ⁶³⁸ ASGTGNMK ⁶⁴⁶ L
<i>ScTPase</i>	4	-PQGGG ²⁹² VALMR	IAFIDD ³⁷⁹ PCM-P	IIYRSH ⁴⁰³ IE---	IAR ⁵⁰⁷ FDPK ⁵¹² GIP	RE ⁶⁰⁶ GFEVKVS ⁶¹⁴ A
<i>EcMalP</i>						
<i>ScTPase</i>						
		$\alpha 6$ (11)	$\beta 12$ (11)	$\beta 13$ (12)	$\beta 19$ (15) $\alpha 18$ (20)	$\alpha 21$ (23)

Figure 6

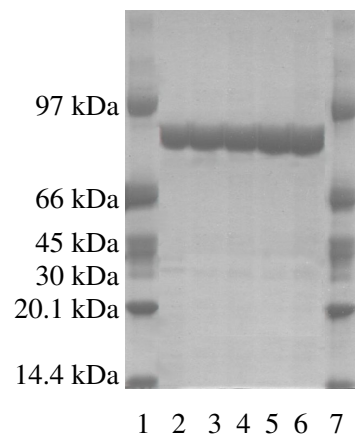


Table 1: Peptide masses obtained by tryptic digestion of intact recombinant *ScTPase* and the two fragmentation products derived from it by spontaneous cleavage. Several peptides of the N-terminal protein part (\approx residues 1 – 200) were detectable in full-length *ScTPase* and the \approx 16-kDa fragment but were missing in the truncated enzyme. #MC, number of missed tryptic cleavage sites; CS, detected charge state; calc. m/z, calculated m/z value for the peptides in the detected charge state; exp. m/z, experimentally acquired m/z value for the peptides in the detected charge state; n.d., not determined.

LC ESI Q-TOF MS				Full-length <i>ScTPase</i>	Truncated <i>ScTPase</i>	~ 16 kDa fraction	
Position	Peptide sequence	#MC	CS	calc. m/z	exp. m/z	exp. m/z	exp. m/z
23 - 33	ASLTNRPTFTK	0	2	618.34	618.39	n.d.	n.d.
97 – 103	HVLDALR	0	2	412.24	412.27	n.d.	412.26
113 - 124	FLGAGITLALLR	0	2	622.89	622.93	n.d.	622.89
163 - 203	ISSTSGSYVPSGAETPTVYVEASHLGNNLSAGTASKLPIPR	1	4	1029.78	1029.87	n.d.	n.d.
189 - 203	NNLSAGTASKLPIPR		2	769.94	n.d.	770.02	n.d.
244 - 255	IHLIDDIDEYRK	1	2	765.40	765.47	765.39	n.d.
513 - 523	GIPNVIDSYAR	0	2	602.82	602.85	602.79	n.d.
731 – 737	GGIKVQD	1	1	716.39	716.46	716.39	n.d.

Table 2: Kinetic parameters and inhibition constants of *Sc*TPase. Reported values for the recombinant enzyme are from non-linear fits of initial rates to the appropriate equations for an ordered bi-bi kinetic mechanism (see Figure 2A) and binding of a competitive inhibitor, as described elsewhere in detail [9, 14, 15]. Values for the native *Sc*TPase are taken from the literature [10, 14]. k_{cat} is the catalytic centre activity calculated by using a subunit molecular mass of 82.8 and 61 kDa for recombinant and natural *Sc*TPase, respectively; K_m is the Michealis constant; K_i is an apparent dissociation constant and K_{ic} is a competitive inhibitor binding constant. Data were recorded at pH 6.6 and 30 °C. The internal consistency of the kinetic parameters was checked with the Haldane relationship, and the calculated and experimentally determined values of the equilibrium constant K_{eq} [9] are in reasonable agreement.

Kinetic properties	Recombinant <i>Sc</i> TPase	Natural <i>Sc</i> TPase
Phosphorolysis		
K_m phosphate [mM]	0.8 ± 0.1	1.4 ± 0.3
K_i phosphate [mM]	12 ± 3	26 ± 4
K_m α,α -trehalose [mM]	53 ± 4	71 ± 5
k_{cat} [s^{-1}]	16.4 ± 0.4	13.3 ± 0.6
K_{ic} vanadate [μM]	0.40 ± 0.11	0.75 ± 0.10
Synthesis		
K_m α -D-Glc 1-P [mM]	2.2 ± 0.5	1.6 ± 0.2
K_i α -D-Glc 1-P [mM]	5.9 ± 0.8	5.8 ± 0.9
K_m glucose [mM]	46 ± 8	35 ± 2
k_{cat} [s^{-1}]	14.1 ± 0.6	9.5 ± 0.7
K_{ic} vanadate [μM]	1.3 ± 0.3	1.1 ± 0.1
calculated K_{eq}	0.482	0.154

Table 3: Kinetic comparison of recombinant ScTPase and site-directed mutants thereof.

$k_{\text{cat}}^{\text{P}}$ and $k_{\text{cat}}^{\text{H}}$ are apparent catalytic centre activities for, respectively, phosphorolysis (P) and hydrolysis (H) of 400 mM α,α -trehalose in the presence (P) and absence (H) of 50 mM phosphate recorded at pH 6.6 and 30 °C. They were calculated with a value of 82.8 kDa for the molecular mass of the enzyme subunit.

	Recombinant ScTPase	D379N	H403A	R507A	K512A
$k_{\text{cat}}^{\text{P}}$ [10^{-4} s^{-1}]	160 000	0.88	110	0.39	1.4
$k_{\text{cat}}^{\text{H}}$ for α,α -trehalose [10^{-4} s^{-1}]	3.5	5.6	5.2	5.0	15
ratio (P/H)	46 000	0.16	21	0.08	0.09